Vertical double diffused MOSFET with step HK insulator improving electric field modulation

Baoxing Duan ✉, *Fengyun Xie, Tongtong Shi, Yintang Yang*

Key Laboratory of the Ministry of Education for Wide Band-Gap Semiconductor Materials and Devices, School of Microelectronics, Xidian University, No. 2 South TaiBai Road, Xi'an 710071, Shaanxi, People's Republic of China
✉ *E-mail: bxduan@163.com*

Published in Micro & Nano Letters; Received on 24th August 2018; Revised on 9th October 2018; Accepted on 6th November 2018

A novel step high-*k* metal–oxide–semiconductor field-effect transistor (step HK-MOSFET) is designed with the step high-*k* insulator based on the HK-MOSFET concept for the first time. In the off-state, the step HK insulator enhances the lateral field component in the drift region due to the new electric field peak, which increases the depletion of the drift region and leading to the low specific on-resistance ($R_{on,\ sp}$) of step HK-MOSFET compared with the conventional HK-MOSFET. Meanwhile, the various thicknesses of the HK insulator modulates the vertical electric field distribution in the drift region, which increases the breakdown voltage (BV) of step HK-MOSFET compared with the conventional vertical double diffused MOSFET and HK-MOSFET. The results show that the simulated BV of step HK-MOSFET is increased from 639 V of the conventional HK-MOSFET to 736 V with the same drift region length of 42 μm or decreased the requirement of permittivity for the HK region to 120 ε_0 from 230 ε_0 with the same BV of 600 V.

1. Introduction: An ideal power metal–oxide–semiconductor field-effect transistor (MOSFET) should meet two requirements: sustaining a very high breakdown voltage (BV) when the devices are in the off-state and an ultralow specific on-resistance ($R_{on,\ sp}$) in the on-state to minimise the conduction losses. However, there is a silicon (Si) limit [1] in the conventional power MOSFET limits the application of power MOSFET devices in the field of high-voltage application. To break this Si limit, various solutions had been proposed and applied in the actual product such as super junction (SJ) devices [2–4]. The principle of the SJ devices is to introduce the new lateral electric field in the drift region by the P pillars which assist the depletion of the N pillars to drift region. As a result, the doping concentrations of the SJ MOSFET can be greatly increased and low on-resistance can be achieved compared with the conventional power MOSFET. However, the BV of SJ MOSFET will be decreased if the charges of N and P pillars are imbalanced [5], which leads to the difficulty of SJ MOSFET manufacture. The half-*k* (HK)-MOSFET [6] has been proposed to solve the effect of charge imbalance. The relation between the BV and $R_{on,\ sp}$ of HK-MOSFET is similar to SJ MOSFET and the doping concentrations of HK-MOSFET are easier to control [7]. The HK-MOSFET has many advantages; however, the selection of HK material is difficult. Hafnium(IV) oxide (HfO_2) as the most common HK material is commonly used as gate dielectrics in the complementary MOS [8], but it is not suitable for HK-MOSFET for the low permittivity. The permittivity for HK material used in the HK-MOSFET should be higher than 200 ε_0 [7]. Lead Zirconate Titanate (PZT) and Bismuth Zinc Niobate (BZN) are two materials with the permittivity up to several thousands, but the materials are susceptible to crack due to the annealing process [9].

In this Letter, a new MOSFET with the step HK (HK-MOSFET) is proposed for the first time to optimise the electric field distribution by improving the electric field modulation effect. The new electric field peak has been introduced compared with the conventional HK-MOSFET. The proposed HK-MOSFET decreases the requirements of the permittivity for HK material to 120 ε_0 from 230 ε_0 for conventional HK-MOSFET with the same BV of 600 V. The permittivity of PZT could reach 150 ε_0 without the annealing process. So, PZT becomes a viable material in the proposed structure.

2. Device structure and description: Fig. 1 shows the schematic cross-section of the proposed step HK-MOSFET and the conventional HK-MOSFET. The difference between the conventional HK-MOSFET and step HK-MOSFET is that the uniform sidewall HK region is replaced with a step HK region. When applied reverse bias, for step HK-MOSFET, the new electric field peak is introduced by the step HK region, which optimises the vertical electric field distribution in the drift region.

For comparison, the step HK-MOSFET with BV = 736 V is proposed and compared with the conventional HK-MOSFET with BV = 639 V [7]. All the key parameters for step HK-MOSFET and conventional HK-MOSFET are listed in Table 1.

The key steps of one feasible fabrication method for the proposed step HK-MOSFET are shown in Fig. 2. First, in Fig. 2*a*, Si lateral epitaxial overgrowth over the drift region to form the P-body. Then, arsenic ions implantation is implemented to form N+ regions. Second, in Fig. 2*b*, deep trench etching the P-body and drift region and gap of the trench are filled with HK pillar by the low-pressure chemical vapour deposition. Third, in Fig. 2*c*, etching a deep trench in the middle of HK pillar and filling the gap of the trench with the oxide to the desired depth by deposition. Next, in Fig. 2*d* the trench is filled with the HK material by deposition. Then, in Fig. 2*e*, etching the HK region and to the bottom of the P-body and filling the trench with p+ polySi. Finally, in Fig. 2*f*, etching the P-body and growth of the gate oxide, polySi is then deposited and planarised to form a gate electrode. The source electrode is formed to complete the process of step HK-MOSFET.

3. Results and discussion: Fig. 3 shows the electric field distributions for the conventional HK-MOSFET and step HK-MOSFET at breakdown using Integrated Software Environment-Technology Computer Aided Design (ISE-TCAD) [10]. For step HK-MOSFET, a new electric field peak is introduced near the interface of the step HK region. The new electric field peak can be explained by the two reasons as follows. On the one hand, the device can be regarded as a parallel plate capacitor without considering the effect of internal charge on the electric field. Combined with Gauss's theorem, in the passive field, the electrical displacement (*Y*-direction) relationship at different positions of the device

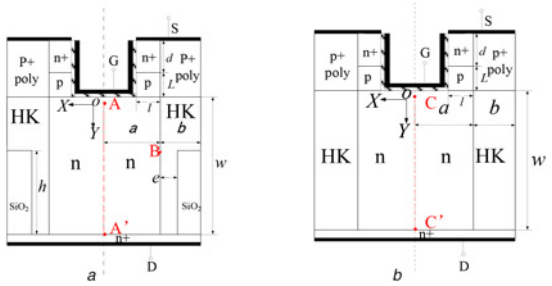

Fig. 1 *Schematic cross-sections of the*
a Step HK-MOSFET
b Conventional HK-MOSFET

can be expressed as in the equation below:

$$\sum^{i} L_{i1} D_{i1} = \sum^{j} L_{j2} D_{j2} \tag{1}$$

where the L_{i1} and L_{j2} are the widths of different dielectrics. For the relative permittivity of HK material is much higher than Si and Si dioxide (SiO_2), most of the electric displacements enter the HK area. Therefore, the electric displacement is inversely proportional to the width of the HK region. With the width of the HK, region decreases from top to bottom, the electric displacement density in the HK region increases which equivalently increases the electric field at the bottom of the drift region. On the other hand, the peak can be explained by solving the Poisson equation as below:

$$\frac{\partial V_S^2(0,\ y)}{\partial y^2} - \frac{V_S(0,\ y)}{\lambda_i^2} = -\frac{\rho}{\varepsilon_{Si}} \tag{2}$$

$$\lambda_i = \sqrt{\frac{1}{2}\left(a^2 + \frac{\varepsilon_{si}}{\varepsilon_I} a t_i\right)} \tag{3}$$

where the V_s is the potential function in the drift region, λ_i is a factor of (2) and t_i is the width of different HK regions. The equation indicates that the electric field can be modulated by the parameters a, t_i and $\boldsymbol{\varepsilon_I}$.

The newly formed electric field peak significantly improves the electric field strength at the bottom of the drift region which is shown in Fig. 3. The electric field distribution of the step HK-MOSFET is modulated to be more uniform compared with the conventional HK-MOSFET, and the BV is increased.

To further explore the characteristics of the new device, the influences of a, b, e, n and $\boldsymbol{\varepsilon_I}$ on the device performance are discussed in this Letter. All data was simulated using ISE-TCAD [10] with a gate voltage of 20 V. On the one hand, the device may break down at point A or point B as shown in Fig. 1*a*. On the other hand, the electric field strength at point B is influenced by the parameters of a, b, e and $\boldsymbol{\varepsilon_I}$. To reach the optimal device performance, the key is to ensure the device breaks down simultaneously at point A and point B.

Fig. 4*a* shows the simulated BV and simulated $R_{on,\ sp}$ versus width of the drift region at the different widths of the HK region. For both step HK-MOSFET and conventional HK-MOSFET, the BV decreases and $R_{on,\ sp}$ increases with the increasing of the width of the drift region. The reason is that electric field modulation weakens as HK region is far away from drift region. When a is <4 μm, the data for $R_{on,\ sp}$ is not shown in Fig. 3*a*. The reason is that the HK region will deplete the sidewall of the drift region nearby. With the a deceases from 4 μm, the conduction channel will be pinched off and the $R_{on,\ sp}$ will increase abruptly. As a result, the device performance reaches optimal when a is 4.2 μm. The BV and $R_{on,\ sp}$ of step HK-MOSFET and conventional HK-MOSFET increase with increasing of the width of the HK region. As the width of the HK region increases, the capacitance area between the drift region and the P region above the HK region increases, which allows more electric displacement lines enter the HK region and improves drift region depletion. With the increasing of b, the relative conduction channel area decreases which increase in the $R_{on,\ sp}$. The optimal of b is about 2.3 μm.

Fig. 4*b* shows the influence of e on BV with different ε_I. For different $\boldsymbol{\varepsilon_I}$ of 300 ε_0, 250 ε_0 and 200 ε_0, the optimal e is 1.3, 1.4 and 1.2 μm, respectively. This is mainly because that the electric field strength at point B increases with the increasing of $\boldsymbol{\varepsilon_I}$ or the decreasing of e. The device will break down at point A and point B simultaneously when e reaches optimum at different $\boldsymbol{\varepsilon_I}$.

The influence of a number of steps on BV with different $\boldsymbol{\varepsilon_I}$ is shown in Fig. 5*a*. BV increases with the increasing of n, and the BV achieves saturation when the number of step HK is three. This is mainly because the electric field will be more uniform with the new peak added and the electric modulation will be saturated at a certain step shape. The influence of the permittivity of HK material on BV with different e is shown in Fig. 5*b*. The BV of step HK-MOSFET is higher than that of conventional HK-MOSFET under the same $\boldsymbol{\varepsilon_I}$ due to a more uniform electric

Table 1 Key parameters for two different HK-MOSFET

Parameters	Definition	Step HK-MOSFET	Conventional HK-MOSFET
ε_I (ε_0)	relative permittivity of HK material	300	300
w, μm	length of the drift region	42	42
a, μm	half of the width of the drift region	4.2	4.2
b, μm	half of the width of the HK material	2.3	2.3
h, μm	length of the step HK material	21	—
e, μm	half of the width of the step HK material	1.5	—
T, nm	gate oxide thickness	30	30
l, μm	width of the channel region	0.1	0.1
d, μm	length of the source region	0.6	0.6
L, μm	length of the p region	1.4	1.4
n	number of step HK materials	1	—
N_D, cm^{-3}	doping of the drift region	2.24×10^{15}	2.24×10^{15}
N_P, cm^{-3}	doping of the p region	2.5×10^{17}	2.5×10^{17}
N_{SOURCE}, cm^{-3}	doping of the source region	2×10^{19}	2×10^{19}
N_{DRAIN}, cm^{-3}	doping of the drain region	1×10^{19}	1×10^{19}
$R_{on,sp}$, mΩ cm^2	specific on-resistance	13.5	13.5
BV, V	BV	736	639

doi: 10.1049/mnl.2018.5501

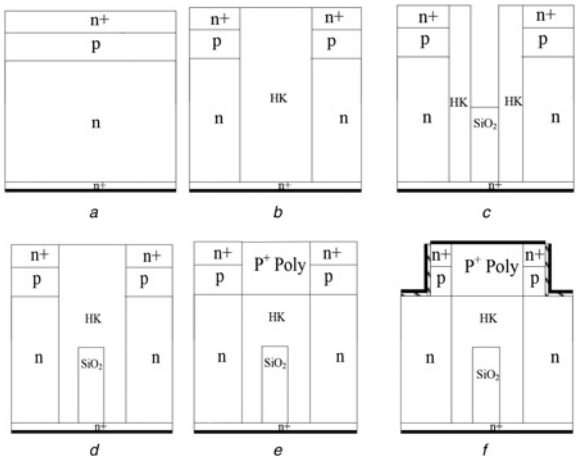

Fig. 2 *Key processes to fabricate step HK-MOSFET*
a Epitaxial overgrowth and ion implantation to form a part of the device
b Deep trench etching and filled the trench with HK pillar
c Deep trench etching the HK pillar and fill the trench with SiO_2
d Fill the trench with HK pillar
e Etching the HK region and fill the trench with p+ polySi
f Etching the P-body and growth the gate oxide, polySi is then deposited and planarised to form a gate electrode, depositing metal to form a source electrode

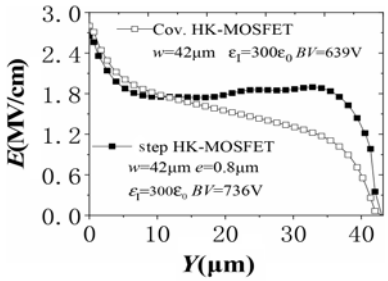

Fig. 3 *Electric field distributions along the vertical direction in the middle of drift regions for step HK-MOSFET and conventional HK-MOSFET*

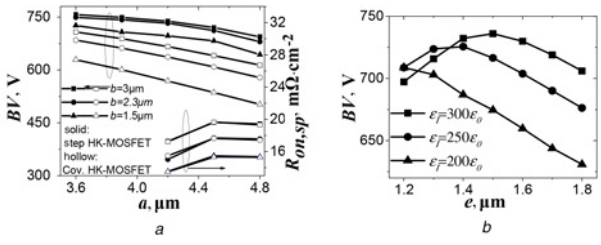

Fig. 4 *Influence of a, b and e on the device performance*
a Dependence of the BV and $R_{on,\ sp}$ on *a* under different *b*
b Dependence of the BV on *e* under different ε_I

field. With the increasing of $\boldsymbol{\varepsilon}_I$ in HK region, BV will be increased continuously, but the degree of the increase will decrease. This shows that the introduction of the HK region helps to improve the relationship between $R_{on,\ sp}$ and BV, but the effect of the HK region will become saturated when the permittivity reaches large enough. Meanwhile, when the BV reaches 600 V rated, the $\boldsymbol{\varepsilon}_I$ for step HK-MOSFET decreases to 120 ε_0 from 230 ε_0 for conventional HK-MOSFET. The lower permittivity requirement means more material can be used for HK-MOSFET.

Fig. 6*a* shows the output characteristics of the conventional HK-MOSFET and step HK-MOSFET. The V_{TH} (threshold voltage) are both about 5 V. At different gate voltages V_g, the

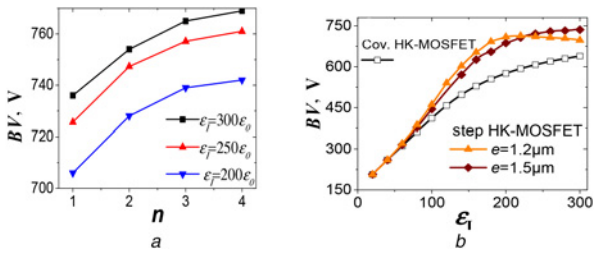

Fig. 5 *Influence of n and ε_I on the device performance*
a Dependence of the BV on *n* under different ε_I
b Dependence of the BV on ε_I under different *e*

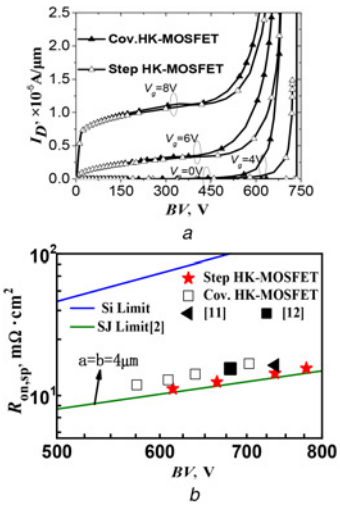

Fig. 6 *$R_{on,\ sp}$ of step HK-MOSFET*
a Output characteristics of the conventional HK-MOSFET and step HK-MOSFET
b $R_{on,\ sp}$ against BV with Si limit line SJ Si limit line and step HK-MOSFET with $a = 4.2$ μm and $b = 2.3$ μm

step HK-MOSFET has a higher BV than that of the conventional HK-MOSFET due to the uniform electric field distribution. With the increase of conduction current density, the BV of the two devices will decrease. This is mainly due to the equivalent negative charge introduced by the conduction current, which increases the doping concentration of the drift region. However, the effect of negative charge will be reduced by the HK regions, and the effect of charge imbalance is not obvious compared with the SJ device. Fig. 6*b* illustrates the simulated $R_{on,sp}$–BV performance of step HK-MOSFET compared with the reported results [9–11]. $R_{on,\ sp}$ of step HK-MOSFET is lower by 15–20% than that of the conventional HK-MOSFET and is close to the SJ MOSFET at the *a* of 4 μm under the optimised conditions.

4. Conclusion: In this Letter, a novel step HK-MOSFET is proposed which replaces the uniform sidewall HK region with a step HK region. The step HK region optimises the vertical electric field distribution based on the HK-MOSFET, which increases the BV. The parameters that affect the BV and specific on-resistance were analysed and optimised by two-dimensional numerical simulations. Results show that the BV of the step HK-MOSFET is 736 V compared with 639 V for the conventional HK-MOSFET with the same permittivity of HK material, increasing by 15%. The permittivity decreases from 230 ε_0 to 120 ε_0 when the BV reaches 600 V rated, the lower permittivity requirement means more material can be used for HK-MOSFET.

5. Acknowledgments: This work was supported by the National Basic Research Program of China (grant no. 2015CB351906), the National Natural Science Foundation of China (grant no. 61774114), the Science Foundation for Distinguished Young Scholars of Shaanxi Province under grant no. 2018JC-017 and 111 Project no. B12026.

6 References

[1] Chen X.B.: 'Breakthrough to the 'silicon limit' of power devices'. Proc. 1998 Fifth Int. Conf. Solid-State and Integrated Circuit Technology, Beijing, China, October 1998, pp. 141–144, doi: 10.1109/ICSICT.1998.785827

[2] Chen X.B., Sin J.K.O.: 'Optimization of the specific on-resistance of the COOLMOS', *IEEE Trans. Electron Devices*, 2001, **48**, (2), pp. 344–348, doi: 10.1109/16.902737

[3] Saremi M., Saremi M., Niazi H.: 'SOI LDMOSFET with up and down extended stepped drift region', *J. Electron. Mater.*, 2017, **46**, pp. 5570–5576, doi: 10.1007/s11664-017-5645-z

[4] Anvarifard M.K.: 'Successfully controlled potential distribution in a novel high-voltage and high-frequency SOI MESFET', *IEEE Trans. Device Mater. Reliab.*, 2016, **16**, pp. 631–637, doi: 10.1109/TDMR.2016.2618850

[5] Shenoy P.M., Bhalla A., Dolny G.M.: 'Analysis of the effect of charge imbalance on the static and dynamic characteristics of the super junction MOSFET'. 1999 Proc. 11th Int. Symp. Power Semiconductor Devices and ICs (ISPSD '99), Toronto, Ontario, Canada, 1999, pp. 99–102, doi: 10.1109/ISPSD.1999.764069

[6] Chen X.B.: 'Super-junction voltage sustaining layers with alternating semiconductor and high-*K* dielectric regions'. U.S. Patent 7230310, 12 June 2007

[7] Chen X.B., Huang M.M.: 'A vertical power MOSFET with an inter-digitated drift region using high-*k* insulator', *IEEE Trans. Electron Devices*, 2012, **59**, pp. 2430–2437, doi: 10.1109/TED.2012.2204890

[8] Zhu W., Ma T.P., Tamagawa T.: 'HfO_2 and HfAlO for CMOS: thermal stability and current transport'. Int. Electron Devices Meet (IEDM), Technical Digest, Washington, D.C., 2001, pp. 463–466, doi: 10.1109/IEDM. 2001.979541

[9] Li J., Li P., Zhang G., *ET AL.*: 'Analysis and fabrication of an LDMOS with high-permittivity dielectric', *IEEE Electron Device Lett.*, 2011, **32**, (9), pp. 1266–1468, doi: 10.1109/LED.2011.2158383

[10] ISE TCAD: 'Manuals release 10.0' (Synopsis Inc., Mountain View, CA, USA, 2004)

[11] Tamaki T., Nakazawa Y., Kanai H., *ET AL.*: 'Vertical charge imbalance effect on 600 V-class trench-filling super junction power MOSFETs'. Proc. ISPSD, San Diego, CA, 23–26 May 2011, pp. 308–311, doi: 10.1109/ISPSD.2011.589085

[12] Saito W., Omura I., Aida S., *ET AL.*: 'A 15.5 $m\Omega\,cm^2$–680 V super-junction MOSFET reduced on-resistance by lateral pitch narrowing'. Proc. ISPSD, Naples, Italy, 4–8 June 2006, pp. 1–4, doi: 10.1109/ISPSD.2006.1666129